

Differential immune responses of 3D gingival and periodontal connective tissue equivalents to microbial colonization

Journal of Tissue Engineering
Volume 13: 1–13
© The Author(s) 2022
Article reuse guidelines:
sagepub.com/journals-permissions
DOI: 10.1177/20417314221111650
journals.sagepub.com/home/tej



Hardik Makkar¹, Srividya Atkuru¹, Yi Ling Tang¹, Tanya Sethi¹,
Chwee Teck Lim², Kai Soo Tan¹ and Gopu Sriram¹ 

Abstract

Gingival and periodontal ligament fibroblasts are functionally distinct cell types within the dento-gingival unit that participate in host immune response. Their microenvironment influences the behavior and immune response to microbial challenge. We developed three-dimensional gingival and periodontal connective tissue equivalents (CTEs) using human fibrin-based matrix. The CTEs were characterized, and the heterogeneity in their innate immune response was investigated. The CTEs demonstrated no to minimal response to planktonic *Streptococcus mitis* and *Streptococcus oralis*, while their biofilms elicited a moderate increase in IL-6 and IL-8 production. In contrast, *Fusobacterium nucleatum* provoked a substantial increase in IL-6 and IL-8 production. Interestingly, the gingival CTEs secreted significantly higher IL-6, while periodontal counterparts produced higher IL-8. In conclusion, the gingival and periodontal CTEs exhibited differential responses to various bacterial challenges. This gives insights into the contribution of tissue topography and fibroblast heterogeneity in rendering protective and specific immune responses toward early biofilm colonizers.

Keywords

3D culture, tissue constructs, fibroblast heterogeneity, innate immune response, periodontopathogens, inflammatory cytokines

Date Received: 16 March 2022; accepted: 20 June 2022

Introduction

The dento-gingival unit that forms a collar around the teeth comprises of epithelial (gingival, sulcular, and junctional) and connective tissue (gingival and periodontal) components.¹ In health, the oral commensals and the host defense mechanism offered by the dento-gingival tissues exist in a state of homeostasis. Dysbiosis in the microflora with the colonization of periodontal pathogens leads to a disruption in the homeostasis, local tissue destruction, and periodontitis.² Along with the epithelium, the gingival and periodontal connective tissues actively participate in innate immune responses against the bacteria in health and diseased states.^{3–6} Despite being covered by gingival epithelium, the gingival, and periodontal connective tissues are not completely sterile even in healthy states. Instead, they are constantly exposed to microbes and/or their products,⁷ which can drive the selective expansion of regional fibroblast

sub-population with differential immune responses.⁸ Hence, it becomes imperative to understand fibroblast heterogeneity within the dento-gingival unit and their immune response to early microbial colonization.

Gingival fibroblasts (GFs) and periodontal ligament fibroblasts (PDLFs) are the primary cell types within the connective tissues of superficial gingival and deeper periodontal tissues, respectively.⁸ Although the GFs and PDLFs are spatially located close to each other and have a similar

¹Faculty of Dentistry, National University of Singapore, Singapore

²Institute for Health Innovation and Technology (iHealthtech), National University of Singapore, Singapore

Corresponding author:

Gopu Sriram, Faculty of Dentistry, National University of Singapore, 9 Lower Kent Ridge Road, Singapore 119085, Singapore.
Email: sriram@nus.edu.sg



spindle-shaped morphology in vitro, they have distinct functional characteristics.^{8–10} GFs and PDLFs are known to produce a variety of pro-inflammatory cytokines, including interleukin (IL)-1 β , IL-6, IL-8, stromal-derived factor (SDF)-1, and tumor necrosis factor-alpha (TNF- α).^{11–14} Interestingly, stimulation of monolayer cultures of GFs and PDLFs with periodontopathogens or their virulence factors like lipopolysaccharide (LPS) demonstrate heterogeneity in their pro-inflammatory cytokine response.^{4,11,14–16} However, much of the literature is based on studies on monolayer cultures, and the findings are conflicting. GFs exposed to LPS from *Porphyromonas gingivalis* (*P. gingivalis*) demonstrated increased SDF-1 and IL-6 compared to PDLFs from the same donor.¹¹ However, exposure to viable *P. gingivalis* induced differential levels of IL-6 and IL-8 production by PDLFs and GFs.⁴ Another study found that GFs exhibited a stronger IL-8 response compared to PDLFs upon stimulation with *Staphylococcus epidermidis* peptidoglycan and muramyl dipeptide.⁵ These studies using monolayer cultures have provided fundamental knowledge on the differential contribution of GFs and PDLFs to the homeostasis and immune response.

There has been growing interest in the application of in vitro three-dimensional (3D) organotypic cultures of reconstructed epithelium,^{17–20} connective tissue,^{21–23} and full-thickness^{6,24–30} equivalents to recapitulate native tissue microenvironment. The 3D culture models have recently enhanced our understanding of the immune response of the gingival epithelium against commensal,^{28,31} intermediate,²⁵ and late^{17,18,20,28} colonizing pathogenic microbiome. However, the isolated response of connective tissues to early microbial colonizers is poorly understood. Secondly, the use of 3D cultures to capture the topological heterogeneity of superficial gingival and deeper periodontal tissues and their immune responses to the oral biofilm colonizers has not been explored.

Therefore, the present study aimed to reconstruct and characterize connective tissue equivalents (CTEs) representative of gingival and periodontal tissues; and investigate their immune response to early microbial colonization represented by oral commensals *Streptococcus mitis* (*S. mitis*), *Streptococcus oralis* (*S. oralis*), and intermediate colonizer *Fusobacterium nucleatum* (*F. nucleatum*).

Methods

Cell culture and fabrication of gingival and periodontal CTEs

Primary PDLFs and GFs were isolated from non-carious human impacted third molars extracted with informed consent from healthy donors following Institutional Review Board approval (No. 2018/00256). The PDLFs were isolated from the tissue fragments scrapped from the middle one-third of the roots. The GFs were isolated from the gingival

tissues attached to the peri-coronal area of the molar tooth. The tissue fragments were cultured as explants in Dulbecco's modified Eagle's medium (DMEM)-low glucose (Gibco) supplemented with 10% fetal bovine serum (Biowest), 1% penicillin-streptomycin (Gibco), and 0.50 μ g/mL amphotericin-B (Gibco). The expanded fibroblasts were cultured under the same media conditions without amphotericin-B, and passage 4–7 were used for the fabrication of the CTEs.

Gingival and periodontal CTEs were fabricated using a fibrin-based hydrogel matrix as previously described.³⁰ Briefly, human fibrinogen (40 mg/mL, Merck Millipore) and polyethylene glycol, succinimidyl glutarate-terminated (PEG, 10 mg/mL, Sigma-Aldrich, 10 kDa) were mixed in a volume ratio of 4:1. After incubation at 37°C for 30 min, the PEG-fibrinogen solution was mixed with fibroblast cell suspension containing 25,000 GFs or PDLFs. The gelation of this mixture was initiated by adding an equal volume of human thrombin (6.25 U/mL, Sigma-Aldrich) in calcium chloride solution (40 mM, Sigma-Aldrich). The constructs (50 μ L in volume) were cultured for 9 days within a low-serum media containing ascorbic acid, hydrocortisone, basic fibroblast growth factor, aprotinin, and 1% penicillin-streptomycin.³⁰ The antibiotics were eliminated from the culture media 3 days before challenge with oral microbes.

Bacterial culture

S. mitis (ATCC 49456), *S. oralis* (ATCC 35037), and *F. nucleatum* (ATCC 25586) strains were purchased from the American Type Culture Collection. *S. mitis* and *S. oralis* were cultured in brain heart infusion (BHI) broth (Acumedia) in a humidified incubator with 5% CO₂ at 37°C. *F. nucleatum* was cultured in BHI broth supplemented with 0.5% yeast extract, 5 μ g/mL hemin (Sigma-Aldrich), and 1 μ g/mL vitamin K, and incubated at 37°C in an anaerobic chamber (Don Whitley Scientific).

Exposure of CTEs to pattern recognition receptor agonists

CTEs were exposed with TLR-2 agonist (Pam3CSK4, Invivogen), and TLR-4 agonist (ultrapure *P. gingivalis* LPS, Invivogen) for 4 and 24 h. Following challenge, the culture supernatants were collected, centrifuged at 5000g for 5 min to remove cellular debris, and the supernatants were stored at –80°C for downstream cytokine analysis.

Bacterial challenge

For the bacterial challenge in planktonic state, the gingival and periodontal CTEs were challenged with the respective microbes (10⁶ CFU/cm²) for 4 and 24 h. To recapitulate post-colonization events, *S. mitis* and *S. oralis* (10⁶ CFU/mL) were cultured on salivary pellicle-coated glass coverslips for 24 h to form biofilm. Before exposure to the CTEs, the biofilms

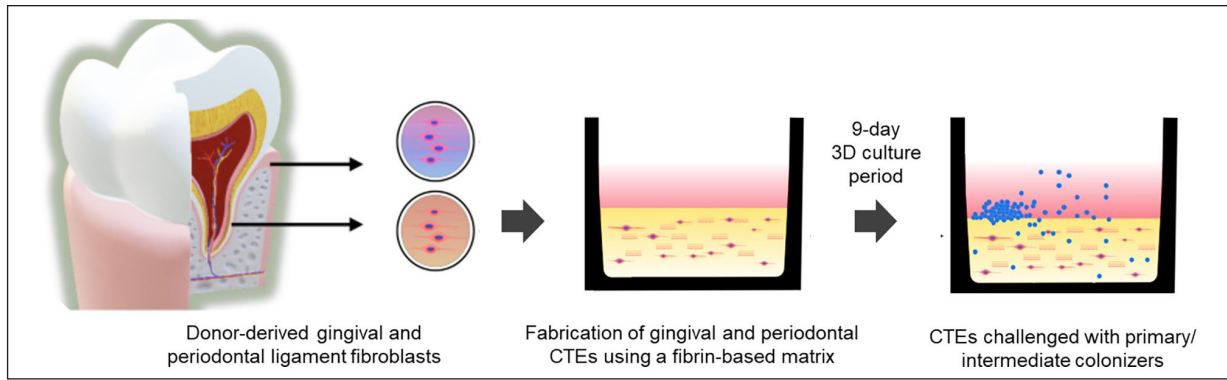


Figure 1. Schematic depicting the workflow for fabrication of gingival and periodontal CTEs and subsequent microbial challenge.

were characterized for viability and biomass. Briefly, the biofilms cultured on coverslips were washed two times with sterile phosphate-buffered saline (PBS) to remove non-adherent bacteria. This was followed by their staining with LIVE/DEAD[®] BacLight[™] bacterial viability kit (Molecular Probes) comprising of SYTO9 (Excitation/Emission 480nm/500nm) and propidium Iodide (Excitation/Emission 490nm/635nm) with the fluorochrome ratio of 1:1. The stained samples were incubated at 37°C for 30 min, gently washed three times with PBS (immersion time per rinse, 3 min) and imaged using laser scanning confocal microscopy (Olympus FluoView[™] FV1000). 3D reconstruction of the z-stacks was performed using Imaris software (Oxford Instruments), and percentage viability and biomass were computed as previously described.^{32,33} Subsequently, for the bacterial challenge in the biofilm state, the coverslips with biofilms were placed on top of the CTEs with the bacterial front facing the tissue and incubated for 24h. After bacterial challenge in planktonic and biofilm state, the culture supernatant was collected, centrifuged to remove cellular debris, and stored at -80°C for downstream cytokine analysis.

Whole-mount visualization using confocal reflectance microscopy

To visualize the collagen and other extracellular matrix (ECM) fibers, whole-mounts of the formalin-fixed CTEs were imaged using laser scanning confocal microscopy (Olympus FluoView[™] FV1000) under reflectance mode as previously described.³⁴ Briefly, the samples were illuminated at 488 nm, and the reflected light was detected with photomultiplier tube detectors. Z-stack images were processed using Fiji/Image J (NIH, USA) and Imaris software (Oxford Instruments).

Histology, immunostaining, and fluorescence in situ hybridization

The CTEs were fixed in 10% neutral-buffered formalin (Sigma-Aldrich), processed, and embedded in paraffin.

Tissue sections (5 μm thick) of formalin-fixed, paraffin-embedded (FFPE) tissues were stained with hematoxylin-eosin (H-E) for histological evaluation.

For immunostaining, the deparaffinized sections were subjected to heat-induced epitope recovery at 121°C in a pressure vessel (Retriever[™] 2100, Aptum Biologics) and 0.01M (pH6) citrate buffer (Sigma-Aldrich). Following blockage of nonspecific staining, the sections were incubated with respective primary antibodies overnight at 4°C. The primary antibodies include rabbit polyclonal anti-collagen-I (Abcam, ab34710, dilution 1:600) and mouse monoclonal anti-vimentin (Novocastra, NCL-VIM-V9, dilution 1:500, Clone V9). Sections were washed, labeled with appropriate secondary antibodies (goat anti-mouse alexa fluor 488 and goat anti-rabbit alexa fluor 594, Molecular Probes) for 45 min, counterstained with DAPI, and mounted with anti-fade fluorescent mounting medium (Abcam). To visualize the bacteria on the CTEs, fluorescence in situ hybridization (FISH) was performed as per manufacturer's specifications (Biovisible BV). Briefly, the deparaffinized and dehydrated tissue sections were hybridized using EUB 338 probe (5'-GCTGCCTCCCGTAGGAGT-3') at 60°C in a humidified chamber for 16h. The slides were washed and mounted for microscopy.

H-E stained slides were visualized using a brightfield microscope (Nikon Eclipse E600 equipped with NIS-Elements software). Immunostained slides were visualized under a fluorescence microscope (Leica DMI8, Leica Microsystems equipped with Leica Application Suite X software) and FISH slides were visualized using laser scanning confocal microscopy (Olympus FluoView[™] FV1000).

Enzyme Linked Immunosorbent Assay (ELISA) for secretome analysis

In accordance with manufacturer's instructions, ELISAs for cytokines IL-1β, IL-6, IL-8, and TNF-α (all from Biologend) were performed using the culture supernatants. The absolute cytokine values were normalized to the total protein content using BCA assay (Thermo Fisher Scientific).

Statistical analysis

All experiments were performed as biological triplicates, and results are presented as mean \pm SD. Statistical significance between groups was determined using ANOVA with Bonferroni corrections and independent t-test using Stata 16 statistical software. Differences were considered significant if $p \leq 0.05$.

Results

Fabrication and characterization of gingival and periodontal CTEs

Donor-derived GFs and PDLFs were characterized for the expression of mesenchymal (CD26, CD44, CD73, CD90, CD105), neural/neural-crest (CD56, CD271) and major histocompatibility complex (HLA-ABC and HLA-DR) markers (Supplemental Figure S1 and Table T1). Results showed that there was no significant difference in the surface marker expression among the two fibroblasts. The GFs and PDLFs were embedded within a human fibrin-based matrix to construct 3D gingival and periodontal CTEs respectively (Figure 1). The fibrin-based matrix was stable, without any visible contraction or degradation over the 9-day culture period. H-E and immunostained sections of the CTEs revealed the presence of vimentin-positive, spindle-shaped fibroblasts that are uniformly distributed within the fibrin matrix (Figure 2(a) and (b)). The fibrin-based matrix provided a natural provisional matrix for the vimentin-positive fibroblasts to produce lamina propria-like ECM. This is evident by the strong expression of cell-derived fibrillar collagen-I in the gingival and periodontal CTEs (Figure 2(a)). Further, whole-mount label-free imaging using confocal reflectance microscopy demonstrated the presence of the fibroblasts within a 3D network of thick cell-derived collagen fibers interspersed with fine collagen fibrils (Figure 2(c) and (d), and Supplemental Videos SV1 and SV2). In most places, the fibroblasts and their cellular processes were embedded within the dense cell-derived collagen network (Figure 2(b)). Amorphous material representative of native fibrin matrix was also seen interspersed between the newly formed collagen fibers. This data correlated well with the immunostaining images wherein a stronger signal of collagen-I was present in the proximity and periphery of the fibroblasts of both gingival and periodontal CTEs. Taken together, these findings suggest matrix remodeling and de novo deposition of collagen-containing ECM by the respective fibroblasts.

CTEs exhibit differential responses to TLR-2 and TLR-4 agonists

Before experiments with bacteria, we investigated the response of gingival and periodontal CTEs to surrogate challenge with TLR-2 (Pam₃CSK₄) and TLR-4 (*P.*

gingivalis LPS) agonists. Both gingival and periodontal CTEs responded by a strong dose and time-dependent increase in the production of IL-6 and IL-8 (Figure 3(a) and (b)). Interestingly, the amount of IL-6 and IL-8 produced by the gingival CTEs was significantly higher than that produced by periodontal CTEs (Figure 3(c)). In contrast, both the CTEs challenged with ultrapure *P. gingivalis* LPS, a TLR-4 agonist did not trigger the production of IL-6 and IL-8 compared to untreated controls (Figure 3(d)–(f)). Transcriptomic studies on monolayer cultures of gingival and periodontal ligament fibroblasts showed expression of TLR-4 mRNA in low abundance ($C_T > 35$, data not shown). These results may explain the absence of immune response to TLR-4 agonist challenge. Overall, the gingival and periodontal CTEs demonstrate a differential pro-inflammatory cytokine response to TLR-2 agonists.

CTEs elicit a heterogeneous innate immune response to planktonic bacteria

We next investigated the innate immune response of gingival and periodontal CTEs to live bacteria (early and intermediate colonizers) exposed in a planktonic state. To recapitulate the initial colonization events, the CTEs were challenged with commensals or primary colonizers *S. mitis* and *S. oralis* and intermediate colonizer *F. nucleatum* in the planktonic state. H-E stained sections showed that the planktonic bacteria had formed biofilm-like structures over the CTEs following the 24h exposure period (Figure 4(a) and (b)). Hybridization with FISH rRNA probe EUB-338 showed the formation of a well-defined layer of bacterial biofilm on top of the CTEs (Figure 4(b)). Serial z-sections demonstrate the thickness of the biofilm and the invasion of some sporadic bacteria into the CTEs (Figure 4(b) and (c)).

The innate immune response of the CTEs was assessed by quantifying the production of IL-1 β , IL-6, IL-8, and TNF- α in the culture supernatants. There was no significant difference in the IL-6 and IL-8 production by gingival CTEs co-cultured with *S. mitis* and *S. oralis* at both 4 and 24h time points (Figure 4(d)). The same was seen in periodontal CTEs except for *S. oralis*, which had triggered a significant IL-8 production after 24h exposure (Figure 4(e)). Both IL-1 β and TNF- α were below the detection limits for all the bacterial exposures studied.

In contrast to the primary colonizers, *F. nucleatum* elicited a time-dependent, significant increase in the IL-6 and IL-8 secretion by both gingival and periodontal CTEs (Figure 4(d) and (e)). IL-6 and IL-8 at 24h time point were over 100-fold compared to the controls and primary colonizers ($p < 0.01$). A comparison of the secretome responses of gingival and periodontal CTEs to *F. nucleatum* showed contrasting trends. Gingival CTEs showed significantly higher IL-6 response, while the periodontal CTEs a significantly higher IL-8 response ($p < 0.05$) (Figure 4(f) and (g)).

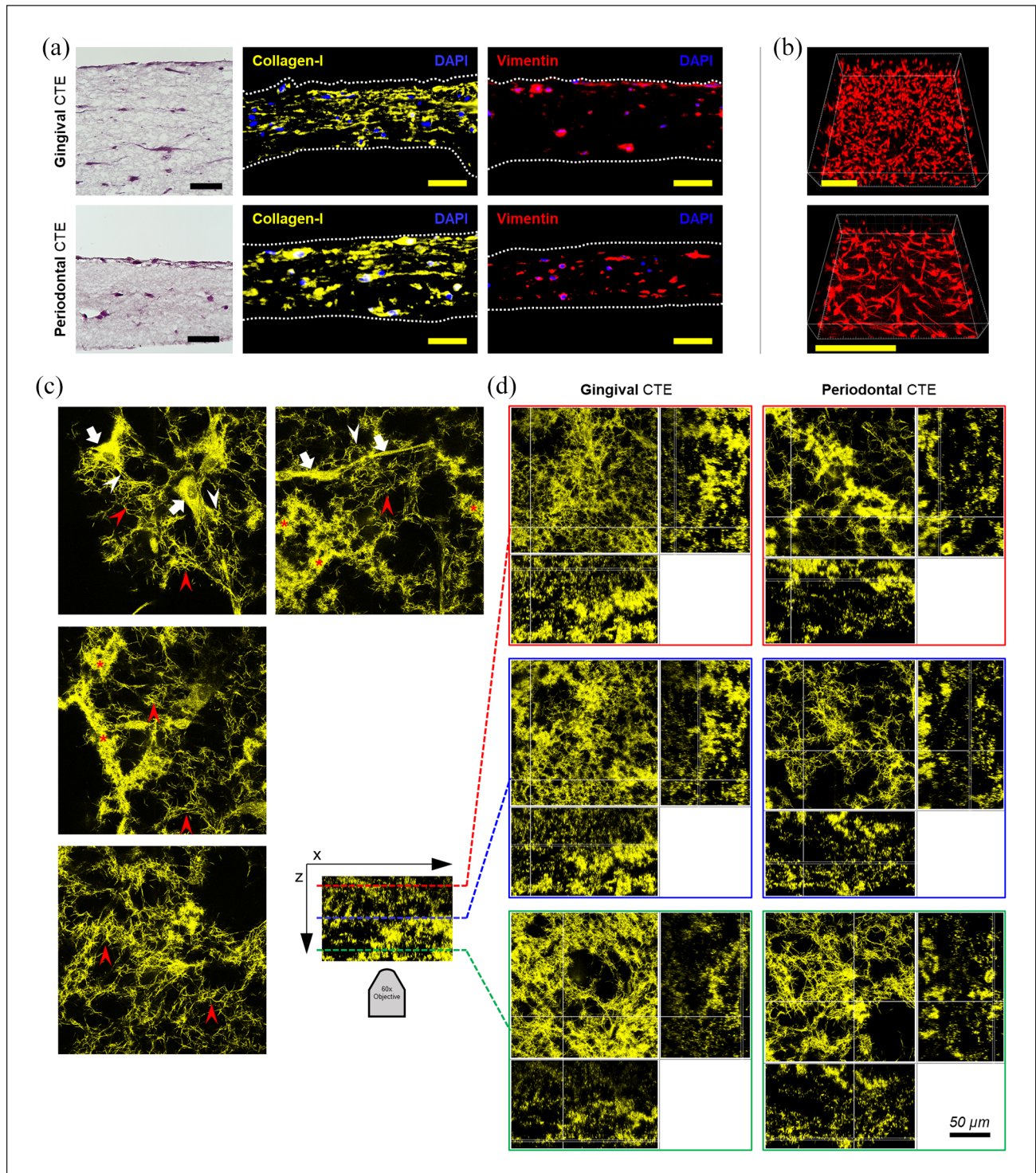


Figure 2. Characterization of connective tissue equivalents (CTEs): (a) H-E and immunostaining of gingival and periodontal CTEs with uniformly distributed, vimentin-positive fibroblasts and cell-derived collagen-I rich extracellular matrix (scale bar-50 μm). (b) Low and high-power magnification of 3D reconstruction of CTEs with CellMask-labeled fibroblasts (scale bar-200 μm). (c) Label-free imaging of CTEs using confocal reflectance microscopy shows cellular and extracellular components that include fibroblasts (white block arrows) surrounded by the newly formed fine network of collagen fibers (red arrowheads). Some collagen fibers could be seen in direct continuity with the fibroblasts (white arrowheads). The amorphous regions (asterisk) interspersed between the collagen fibers represent the remanent fibrin matrix, and (d) XYZ cross-sectional views of confocal z-stack images at different z-levels show the remodeling of the fibrin matrix and dense collagen fiber network formation throughout the matrix (scale bar-50 μm).

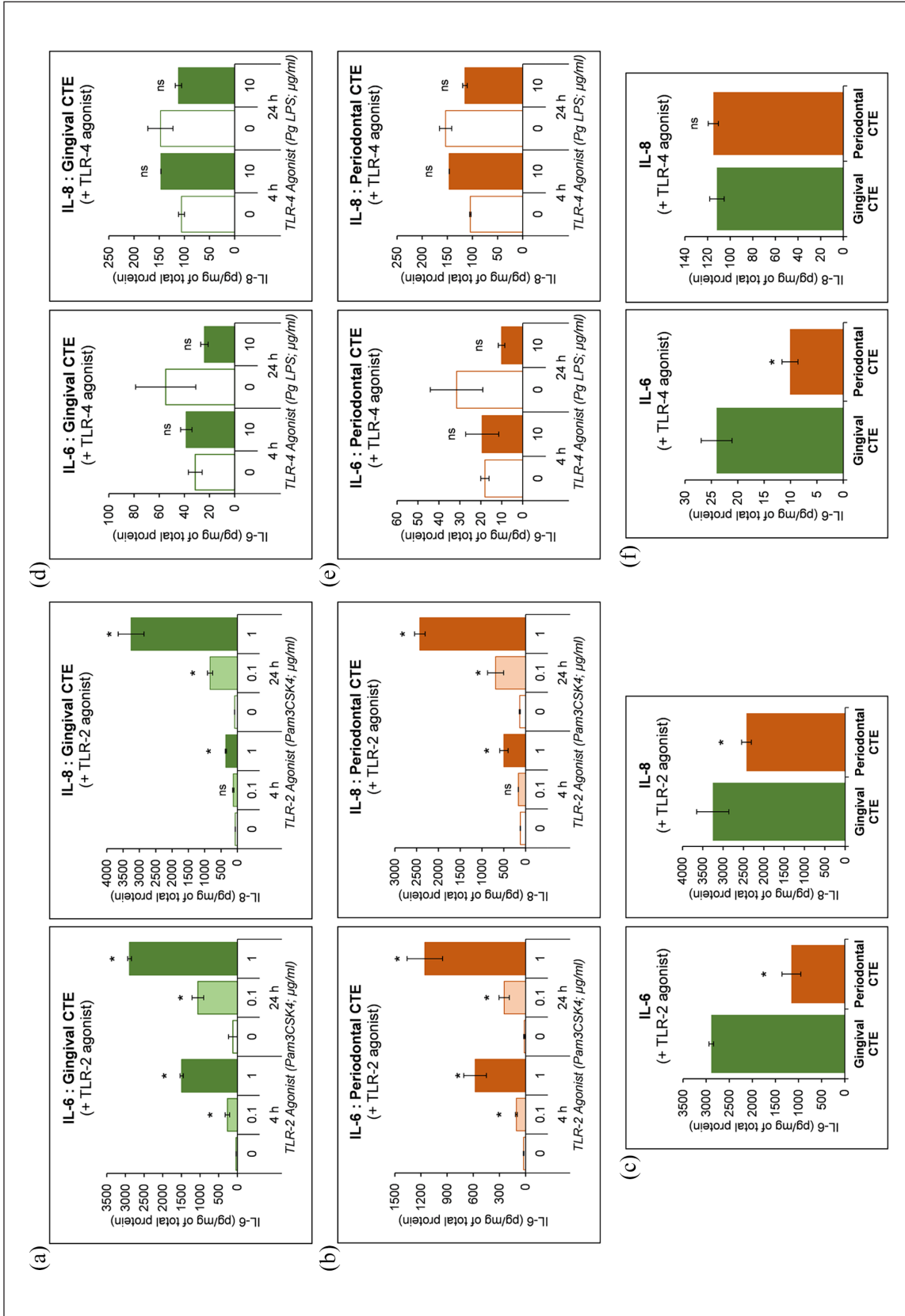


Figure 3. Secretome analysis of connective tissue equivalents (CTEs) exposed to TLR agonists. Graphs showing IL-6 and IL-8 production by gingival (a) and periodontal CTEs (b) after dose- and time-dependent challenge with TLR-2 agonist (Pam3CSK4). Graphs showing IL-6 and IL-8 production by gingival (d) and periodontal CTEs (e) after time-dependent challenge with TLR-4 agonist (*P. gingivalis* LPS). (c and f) Comparisons between CTEs show the differential response in IL-6 and IL-8 secretion when challenged with TLR-2 (1 $\mu\text{g/ml}$) and TLR-4 (10 $\mu\text{g/ml}$) agonist for 24h (Data presented as mean \pm SD, * $p < 0.05$, ** $p < 0.01$, $n = 3$).

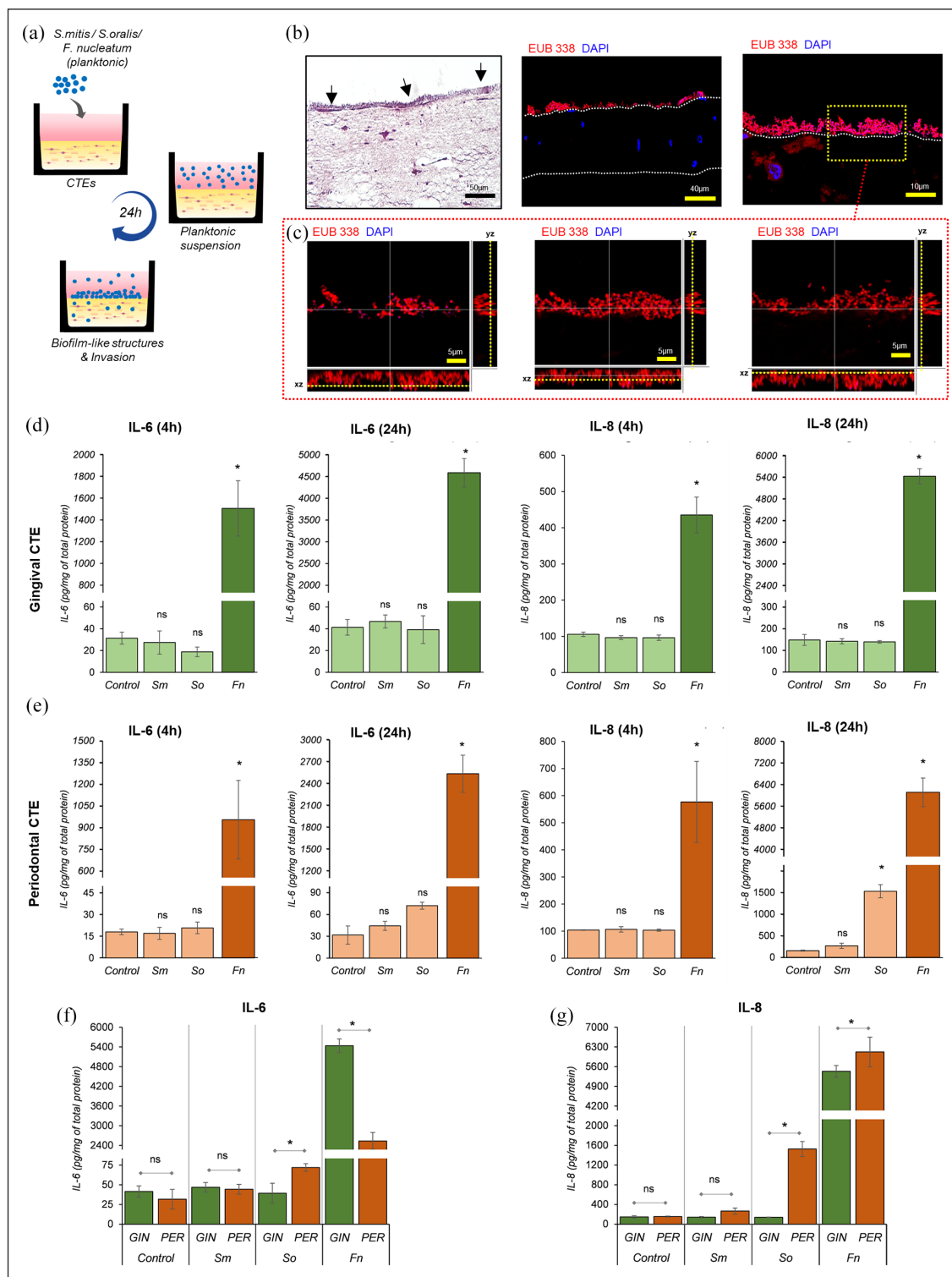


Figure 4. Innate immune response by CTEs after co-culture with bacteria in planktonic state: (a) Schematic representing the exposure of CTEs with primary and intermediate colonizers in planktonic state and formation of biofilm-like clusters on tissue equivalents after 24 h of co-culture, (b) H-E micrographs showing bacterial clusters (black arrows) on the CTEs (scale bar-50 μ m). Representative projections of confocal z-stacks of tissues hybridized by FISH probe EUB 338 shows well-defined biofilm formation of tissue equivalents across the length of the section, (c) A defined area in yellow-dotted rectangle is shown as a series of confocal z-stack images from the top to the bottom of the stacks. The cross-hair lines denote XZ and YZ projections (scale bar-5 μ m). Series of bar graphs show the IL-6 and IL-8 secretion by gingival (d) and periodontal (e) CTEs after 4 and 24 h of co-culture with Sm, So, and Fn. (f and g) Comparisons between the gingival and periodontal CTEs shows the contrasting response in IL-6 (f) and IL-8 (g) secretion after co-culture with primary (Sm, So) and intermediate (Fn) colonizers in the planktonic state for 24 h (Data presented as mean \pm SD, * $p < 0.05$, ** $p < 0.01$, $n = 3$). Sm—*S. mitis*, So—*S. oralis*, Fn—*F. nucleatum*.

Overall, these results show the contrasting cytokine response of gingival and periodontal CTEs to primary and intermediate colonizers in the planktonic state.

Gingival and periodontal CTEs elicit differential immune responses to bacterial biofilms

We next investigated the immune response of the two CTEs to bacterial biofilms post-colonization, wherein the cultures were exposed to 24h-old biofilms (Figure 5(a)). The total biomass of the microbial biofilms computed based on the 3D reconstruction of confocal z-stack images showed similar biomass across all bacterial species (Figure 5(b) and (c)). Viability assessment of bacterial biofilms of *S. mitis* and *S. oralis* after 24-h culture showed ~80% viability (Figure 5(c)). Following the biofilm formation, they were placed on top of the CTEs for a 24h challenge period. Confocal z-stacks of the tissues hybridized with FISH rRNA probe EUB-338 showed the presence of adherent biofilm over the exposed surface of the CTEs and some sporadic bacteria invading the matrix (Figure 5(d) and (e)).

In contrast to the planktonic state, the CTEs exposed to primary colonizers in the biofilm elicited a moderate immune response demonstrated by significant secretion of IL-6 and IL-8 (Figure 5(f)). However, the IL-6 and IL-8 levels were significantly lower than that elicited by *F. nucleatum* ($p < 0.05$). We also noticed a differential innate immune response by the CTEs, wherein the gingival CTEs secreted significantly higher IL-6 and periodontal CTEs higher IL-8 levels upon exposure to streptococcal biofilms (Figure 5(f)). Overall, the higher and differential cytokine secretion by the two CTEs in response to streptococcal biofilms, demonstrate the heterogeneity between gingival and periodontal connective tissues.

Discussion

This study presents a method to fabricate 3D gingival and periodontal CTEs using a human fibrin-based matrix and investigate the heterogeneity in their innate immune response to early microbial colonization. To understand the host-microbiome interaction of the CTEs, an in vitro infection model employing a range of bacterial challenges that include surrogate TLR-2 and TLR-4 agonists, commensal bacteria (*S. mitis* and *S. oralis*), and intermediate colonizers (*F. nucleatum*) were used. Although the GFs and PDLFs were isolated from the same donors and topographically close locations, they exhibited diverse responses to bacterial challenges that recapitulated the regional fibroblast heterogeneity. The CTEs exhibited a heterogeneous response to commensal bacteria depending on planktonic and biofilm states. Oral streptococci in the planktonic state triggered no to mild innate immune response, while streptococcal biofilms elicited a moderate immune response characterized by the production of

higher amount of pro-inflammatory cytokines IL-6 and IL-8. In contrast, exposure to *F. nucleatum* elicited a strong and differential production of IL-6 and IL-8 by the two CTEs. The gingival CTEs representative of superficial connective tissue produced a higher pro-inflammatory and mitogenic cytokine IL-6. In contrast, the deeper connective tissue (periodontal CTEs) predominantly responded through higher production of IL-8, a chemokine involved in immune cell chemotaxis and angiogenesis (Figure 6).

Exposure of GFs and PDLFs cultured as monolayers are commonly used for host-microbiome studies, till date. They are the simplest models, easy to setup, and effective for mechanistic studies. However, the results from monolayer culture models may not represent the features of complex 3D cell-cell and cell-matrix interactions³⁵ and their impact on the tissue response to bacterial challenge. Therefore, in this study, we developed a 3D culture model to represent the gingival and periodontal connective tissue elements of the dento-gingival unit, respectively. ECM is an integral component of connective tissue and the host cellular microenvironment. Collagen-based matrices (typically from rat-tail and bovine origin) are commonly used for the fabrication of 3D cultures.^{22,23,36} However, it has technical and translational limitations owing to its contractile nature and xenogeneic origin.³⁶ Contraction of the collagen gels due to polymerization and fibroblast-mediated process raises technical concerns on reproducibility and long-term cultures.³⁶ Polymeric scaffolds are thus commonly used to counteract the contraction and handling issues with collagen matrices.²¹ Unlike commonly used collagen matrices,^{22,36} the human fibrin-based matrix used in this study was stable without any visible contraction or degradation issues, thus enabling culture over a long period. Non-invasive and label-free imaging using confocal reflectance microscopy supplemented with immunostaining for collagen-1 revealed that the GFs and PDLFs deposited de novo cell-derived collagen and ECM fibers.

The ECM plays a critical role in providing substrate for microbial adhesion and penetration in the host. There is growing evidence that various ECM components and their degradation products also contribute to tissue inflammation and innate immune response to microbial pathogens.^{37,38} ECM components and degradation products of collagen, glycoproteins (e.g. fibrinogen, fibronectin, tenascin-C), proteoglycans (e.g. aggrecan, biglycan, decorin, versican), and glycosaminoglycans (e.g. hyaluronan, heparan sulfate) which can be potentially released from damaged tissues have been identified as capable of acting as danger-associated molecular patterns.³⁷ Hence, the choice of ECM components used to fabricate 3D tissue equivalents can potentially impact the innate immune response against microbial pathogens. For instance, low molecular weight hyaluronic acid has been shown to activate TLR-2 signaling, while its high molecular counterpart inhibits TLR-2 signaling.³⁹ Similarly, fibrin and its

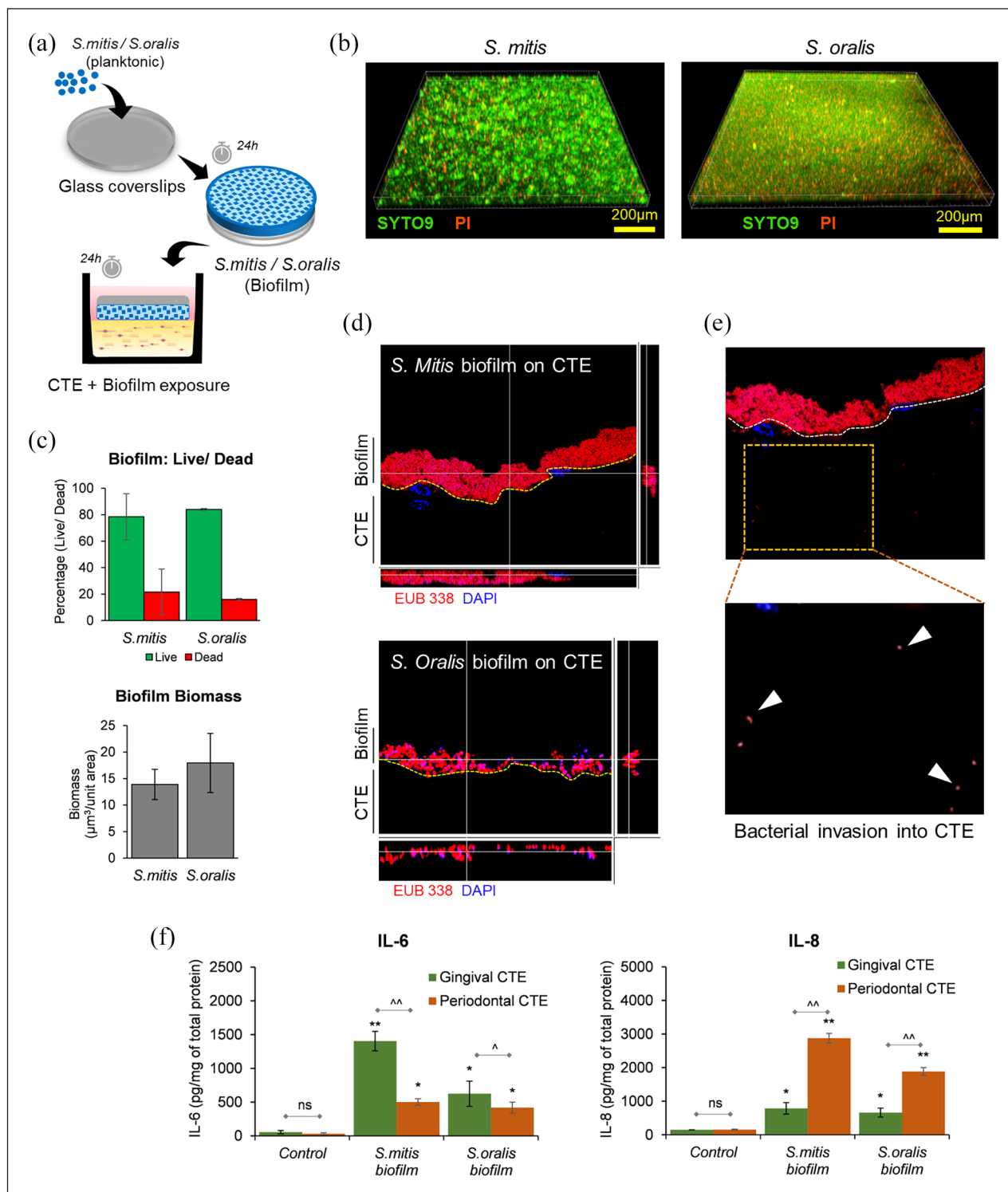


Figure 5. Response by CTEs after exposure with commensal biofilms and the impact of tissue heterogeneity: (a) Schematic showing method employed to culture *S. mitis* (*Sm*) and *S. oralis* (*So*) biofilm and exposure to CTEs for 24 h. (b) 3D reconstruction of the confocal z-stack images of mono-species biofilm of *S. mitis* and *S. oralis* stained with SYTO-9 and PI. (c) Graphs showing percentage viability and biomass of mono-species biofilms. (d) Confocal z-stack images of hybridized sections of CTEs with FISH probe EUB 338 exposed to *S. mitis* and *S. oralis* biofilms showing the portion of the biofilm adhered to tissue equivalents. (e) Enlarged view of sections shows localized bacterial invasion (white arrowheads) of the CTEs. (f) Graphs showing IL-6 and IL-8 secretion by gingival and periodontal CTEs exposed to commensal (*S. mitis* and *S. oralis*) biofilms. Data presented as mean \pm SD, compared to respective control (* $p < 0.05$ and ** $p < 0.01$), comparison between gingival and periodontal CTEs ($\wedge p < 0.05$ and $\wedge\wedge p < 0.01$), $n = 3$.

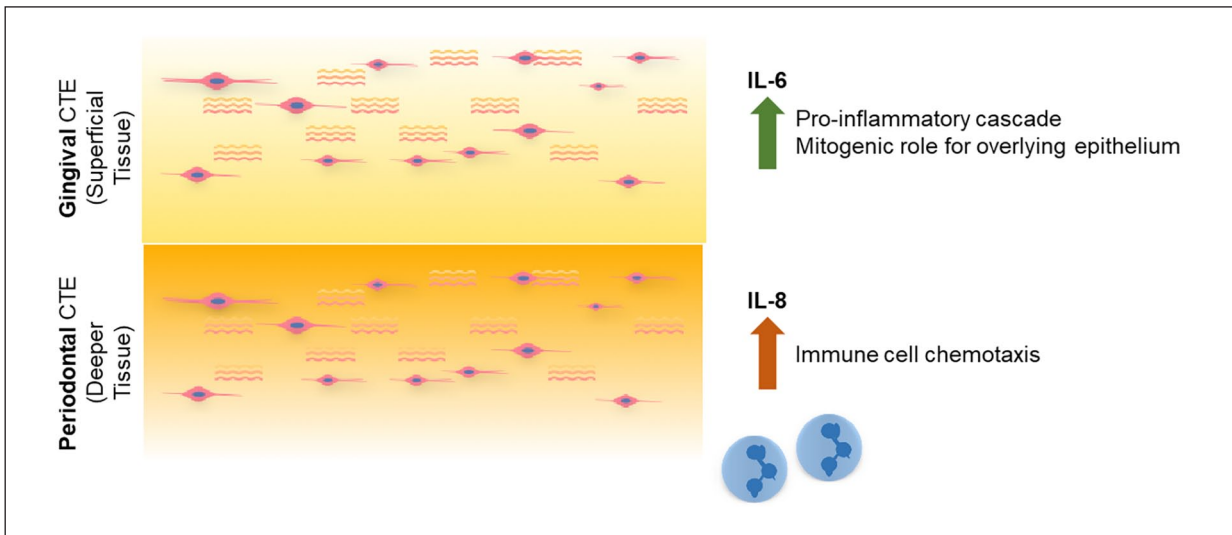


Figure 6. Schematic shows that tissue topography influences immune responses to early colonizers wherein the superficial connective tissue (gingival CTE) responds through higher pro-inflammatory cytokine IL-6 secretion and the deeper connective tissue (periodontal CTE) through higher IL-8 production.

precursor fibrinogen have been demonstrated to display differential regulation of macrophages upon stimulation with LPS and interferon- γ .⁴⁰ Macrophages cultured on fibrin gels displayed an anti-inflammatory phenotype (increased production on IL-10 and decreased levels of tumor necrosis factor alpha), while its precursor fibrinogen stimulated inflammatory activation. Future studies on the impact of various ECM components and their degradation products (in response to host or bacterial proteases) on the innate immune response against periodontopathogens can provide insights on developing ECM-based immunomodulatory strategies.^{41,42}

The in vitro infection of CTE models used in this study, enabled the potential to recapitulate spatiotemporal early microbial colonization by planktonic oral commensals. The planktonic oral commensals formed well-defined biofilm-like structures over the tissues after 24 h of co-culture. Alternatively, as demonstrated in this study and others,^{27–29,43} the 3D organotypic tissues could be challenged with preformed bacterial biofilms. The 3D architecture of organotypic cultures also offers the advantage of visualizing microbial adhesion, biofilm formation, and microbial invasion.^{28,29} The bacterial challenge in the form of both live planktonic and biofilm states used in this study and studies using organotypic gingival epithelium,^{27–29,43} results in the recapitulation of the host-microbiome interface of native gingival and periodontal tissues (albeit without the overlying gingival epithelium). In contrast, host-microbiome studies on monolayer cultures are typically based on exposure of microbiome in planktonic states using multiplicity of infection or CFU/mL.^{4,16,44} However, exposure on 3D culture models offer the potential for exposure based on surface area and as microbial biofilms.

This precludes the ability for direct comparison of the cellular responses between monolayer and 3D culture systems.

Previous studies using monolayer cultures of GFs and PDLFs and gene expression or microarray analysis have demonstrated the heterogeneity in constitutive expression of various genes, including inflammatory cytokines among the two cell types.^{8,11–14,45} Further, this translates to contrasting cytokine responses of the GFs and PDLFs to periodontopathogens like *P. gingivalis* or its virulence factors like LPS.^{4,11,14–16} Similarly, previous studies have demonstrated the differential innate immune response of monolayer cultures of gingival keratinocytes and fibroblasts to periodontopathogens.^{46,47} Gingival keratinocytes exposed to periodontopathogens expressed higher levels of IL-1 β and IL-8, but not IL-6 transcripts. However, GFs exhibited upregulation in IL-6 and IL-8 but not IL-1 β transcripts.⁴⁷ Further, periodontopathogens elicit a higher IL-8 secretion among GFs than oral epithelial cells.⁴⁶ Some studies attribute the differential responses could be due to differences in the expression levels of pattern recognition receptors (PRRs) like the TLRs, among the different cell types and among different donors.^{4,5,48} However, exact mechanisms driving the heterogeneity in the response to bacteria and their products is poorly understood.

Previous studies have demonstrated the involvement of TLR and nucleotide-binding oligomerization domain (NOD)-containing protein-like receptors (NLR) signaling pathways to mediate the innate immune response through the production of cytokines like IL-6 and IL-8.^{5,43,48–52} TLRs are a family of membrane-associated PRRs that lead to the activation of nuclear factor kappa B (NF- κ B), interferon regulatory factors (IRF), and mitogen-activated

protein kinases (MAPK) signaling pathways.^{43,52,53} On the other hand, NLRs are located in the cytoplasm, and are predominantly activated through bacterial invasion into the cells. Activation of intracellular NOD1 and(or) NOD2 in GFs and PDLFs could mediate the release of IL-6 and IL-8 through the activation of NF- κ B and MAPK signaling pathways.⁴⁹ In the present study, exposure to TLR-2 agonist triggered a significantly higher IL-6 and IL-8 among gingival CTEs than its periodontal counterpart. On the contrary, we did not observe any immune response by both CTEs exposed to TLR-4 agonist (ultrapure *P. gingivalis* LPS) despite its high dose (10 μ g/mL). Though transcriptomic studies did not show the expression of *TLR-4* mRNA in GFs and PDLFs (data not shown), the lack of response could also be related to the TLR-4 agonist used in this study. Behm et al.⁵⁴ demonstrated the heterogeneity in the response of gingival and periodontal mesenchymal stromal cells (MSCs) to standard and ultrapure preparations of *P. gingivalis* LPS. Both the MSCs showed a lower immune response to ultrapure *P. gingivalis* LPS compared to the standard preparations. It was attributed to the presence of trace amounts of lipoproteins in standard LPS preparations that activates TLR-2 response in addition to TLR-4 mediated response. In contrast, the enzymatic treatment employed in the preparation of ultrapure LPS leads to degradation of the lipoproteins and hence, to a pure TLR-4 mediated response.

In this study, the exposure of gingival and periodontal CTEs to oral commensals in the planktonic state triggered a none to mild innate immune response. In contrast to *S. mitis*, CTEs exposed to planktonic *S. oralis* induced significantly higher IL-8 secretion after 24 h of exposure. Though both the oral streptococci are known producers of hydrogen peroxide as a by-product of bacterial metabolism, previous work has shown this effect to be relatively higher in the case of *S. oralis*.⁵⁵ This may have attributed towards the overwhelming of the antioxidant defense system of the CTEs, potentially activating the redox sensitive transcription factor (e.g. NF- κ B), and eliciting the production of chemokine IL-8.^{56,57} In contrast, challenges with commensal (streptococcal) biofilms elicited a moderate immune response characterized by the production of inflammatory cytokines IL-6 and IL-8. However, the levels were significantly lower than in response to *F. nucleatum*. Lactate dehydrogenase activity showed minimal impact of the streptococcal biofilms or *F. nucleatum* on cytotoxicity, and hence, it is unlikely due to cell death and the associated release of intracellular cytokines (Supplemental Figure S2). It is plausible that the moderate degree of inflammation elicited by the commensal bacteria could help to prime the tissues against potential attack from pathogens.⁷ In particular, the increased production of inflammatory cytokines by gingival connective tissues could be involved in the induction of an anti-microbial protective response in the overlying gingival epithelium through stimulation of epithelial proliferation and migration.^{18,28,29} These observations

correspond with the microenvironment observed in the oral cavity, where the commensal microbial population keeps the gingiva in a mildly activated state. This helps the host to counter the pathogenic challenge and maintain homeostasis.⁷ In the present study, exposure to commensal biofilms also triggered the production of chemokine IL-8 by both gingival and periodontal CTEs. IL-8 has a crucial role in maintaining a clinically healthy junctional epithelium by promoting immune cell chemotaxis.²⁰ This potentially keeps the periodontium on alert state and primes the tissues to prevent further assault by periodontal pathogens. Previous studies on full-thickness gingiva equivalents have also shown the production of protective cytokine and chemokines by reconstructed tissues when co-cultured with commensal bacterial biofilms.²⁸ The interaction with commensal bacterial biofilms also promoted an increased proliferation and stratification of the gingival epithelium, thus initiating a protective response of the barrier tissues.²⁹ In concordance, the present study also showed that gingival CTEs exposed to commensal biofilm produced higher secretion of pleiotropic cytokine IL6 which is also known to regulate epithelial proliferation.⁵⁸

Future studies on exposure of the CTEs to pathogenic biofilms, particularly from diseased sites, could help provide a deeper understanding of the priming ability of commensals and immune evasion strategy of pathogens. Further, to mimic the microphysiology, it would be beneficial to investigate the response of the CTEs primed by commensal biofilms before exposure to pathogenic biofilms. However, such a setup would require a prolonged culture period, which may not be feasible in the current 3D culture system due to bacterial overgrowth and nutrient depletion. Next-generation tools like microfluidic organ-on-chip systems provide the opportunities to continuously perfuse the tissues for better nutrient delivery and drainage of metabolic wastes.⁵⁹ Further, the microfluidic channels and compartmentalization can enable the potential to introduce different bacterial challenges at desired time points and over the long-term culture period.^{60,61} Microfluidic gut-on-chip models have demonstrated the ability to model and study long-term host-microbiome interactions between intestinal bacteria and gut mucosa.⁶⁰ One of the limitations of our model is the lack of immune cells that help to amplify and translate the innate immune response of the connective tissues. Microfluidic systems that incorporate or present the immune cells at defined time points can also biomimic the recruitment and migration of immune cells into the tissue.^{62,63} Future studies combining the 3D culture and microfluidic systems can be transformative and provide novel insights into host-microbial interactions and opportunities to develop novel therapeutic strategies.

Declaration of conflicting interests

The author(s) declared no potential conflicts of interest with respect to the research, authorship, and/or publication of this article.

Funding

The author(s) disclosed receipt of the following financial support for the research, authorship, and/or publication of this article: This work was supported by grants from iHealthtech Microbiome Seed Grant (A-0002947-00-00, A-0002947-01-00), and Singapore Ministry of Education Academic Research Fund Tier 1 (A-0002090-00-00; A-0002084-00-00). Hardik Makkar is supported by President Graduate Fellowship, and Srividya Atkuru is supported by NUS Research Scholarship.

ORCID iD

Gopu Sriram  <https://orcid.org/0000-0001-8423-5197>

Supplemental material

Supplemental material for this article is available online.

References

- Kurgan S and Kantarci A. Molecular basis for immunohistochemical and inflammatory changes during progression of gingivitis to periodontitis. *Periodontol* 2000 2018; 76: 51–67.
- Bosshardt DD. The periodontal pocket: pathogenesis, histopathology and consequences. *Periodontol* 2000 2018; 76: 43–50.
- Bosshardt DD and Lang NP. The junctional epithelium: from health to disease. *J Dent Res* 2005; 84: 9–20.
- Scheres N, Laine ML, de Vries TJ, et al. Gingival and periodontal ligament fibroblasts differ in their inflammatory response to viable *Porphyromonas gingivalis*. *J Periodontal Res* 2010; 45: 262–270.
- Hatakeyama J, Tamai R, Sugiyama A, et al. Contrasting responses of human gingival and periodontal ligament fibroblasts to bacterial cell-surface components through the CD14/Toll-like receptor system. *Oral Microbiol Immunol* 2003; 18: 14–23.
- Lu EM, Hobbs C, Dyer C, et al. Differential regulation of epithelial growth by gingival and periodontal fibroblasts in vitro. *J Periodontal Res* 2020; 55: 859–867.
- Devine DA, Marsh PD and Meade J. Modulation of host responses by oral commensal bacteria. *J Oral Microbiol* 2015; 7: 26941.
- Lekic PC, Pender N and McCulloch CA. Is fibroblast heterogeneity relevant to the health, diseases, and treatments of periodontal tissues? *Crit Rev Oral Biol Med* 1997; 8: 253–268.
- McKnight H, Kelsey WP, Hooper DA, et al. Proteomic analyses of human gingival and periodontal ligament fibroblasts. *J Periodontol* 2014; 85: 810–818.
- Palaiologou AA, Yukna RA, Moses R, et al. Gingival, dermal, and periodontal ligament fibroblasts express different extracellular matrix receptors. *J Periodontol* 2001; 72: 798–807.
- Morandini AC, Sipert CR, Gasparoto TH, et al. Differential production of macrophage inflammatory protein-1 α , stromal-derived factor-1, and IL-6 by human cultured periodontal ligament and gingival fibroblasts challenged with lipopolysaccharide from *P. Gingivalis*. *J Periodontol* 2010; 81: 310–317.
- Ara T, Kurata K, Hirai K, et al. Human gingival fibroblasts are critical in sustaining inflammation in periodontal disease. *J Periodontal Res* 2009; 44: 21–27.
- Bozkurt SB, Hakki SS, Hakki EE, et al. *Porphyromonas gingivalis* lipopolysaccharide induces a pro-inflammatory human gingival fibroblast phenotype. *Inflammation* 2017; 40: 144–153.
- Kang W, Hu Z and Ge S. Healthy and inflamed gingival fibroblasts differ in their inflammatory response to *Porphyromonas gingivalis* lipopolysaccharide. *Inflammation* 2016; 39: 1842–1852.
- Nilsson B. Mechanisms involved in regulation of periodontal ligament cell production of pro-inflammatory cytokines: implications in periodontitis. *J Periodontal Res* 2021; 56: 249–255.
- Scheres N, Laine ML, Sipos PM, et al. Periodontal ligament and gingival fibroblasts from periodontitis patients are more active in interaction with *Porphyromonas gingivalis*. *J Periodontal Res* 2011; 46: 407–416.
- Thurnheer T, Belibasakis GN and Bostanci N. Colonisation of gingival epithelia by subgingival biofilms in vitro: role of “red complex” bacteria. *Arch Oral Biol* 2014; 59: 977–986.
- Bostanci N, Bao K, Wahlander A, et al. Secretome of gingival epithelium in response to subgingival biofilms. *Mol Oral Microbiol* 2015; 30: 323–335.
- Azuma MM, Balani P, Boisvert H, et al. Endogenous acid ceramidase protects epithelial cells from *Porphyromonas gingivalis*-induced inflammation in vitro. *Biochem Biophys Res Commun* 2018; 495: 2383–2389.
- Belibasakis GN, Thurnheer T and Bostanci N. Interleukin-8 responses of multi-layer gingival epithelia to subgingival biofilms: role of the “red complex” species. *PLoS One* 2013; 8: e81581.
- Hillmann G, Gebert A and Geurtsen W. Matrix expression and proliferation of primary gingival fibroblasts in a three-dimensional cell culture model. *J Cell Sci* 1999; 112(17): 2823–2832.
- Chaussain Miller C, Septier D, Bonnefoix M, et al. Human dermal and gingival fibroblasts in a three-dimensional culture: a comparative study on matrix remodeling. *Clin Oral Invest* 2002; 6: 39–50.
- Oberoi G, Janjić K, Müller AS, et al. Contraction dynamics of rod microtissues of gingiva-derived and periodontal ligament-derived cells. *Front Physiol* 2018; 9: 1683.
- Gursoy UK, Pöllänen M, Könönen E, et al. A novel organotypic dento-epithelial culture model: effect of *Fusobacterium nucleatum* biofilm on B-defensin-2, -3, and LL-37 expression. *J Periodontol* 2012; 83: 242–247.
- Pöllänen MT, Gursoy UK, Könönen E, et al. *Fusobacterium nucleatum* biofilm induces epithelial migration in an organotypic model of dento-gingival junction. *J Periodontol* 2012; 83: 1329–1335.
- Pinnock A, Murdoch C, Moharamzadeh K, et al. Characterisation and optimisation of organotypic oral mucosal models to study *Porphyromonas gingivalis* invasion. *Microbes Infect* 2014; 16: 310–319.
- Ingendoh-Tsakmakidis A, Mikolai C, Winkel A, et al. Commensal and pathogenic biofilms differently modulate peri-implant oral mucosa in an organotypic model. *Cell Microbiol* 2019; 21: e13078.
- Buskermolen JK, Janus MM, Roffel S, et al. Saliva-derived commensal and pathogenic biofilms in a human gingiva model. *J Dent Res* 2017; 97: 201–208.

29. Shang L, Deng D, Buskermolen JK, et al. Multi-species oral biofilm promotes reconstructed human gingiva epithelial barrier function. *Sci Rep* 2018; 8: 16061.
30. Sriram G, Sudhakaran T and Wright GD. Multiphoton microscopy for noninvasive and label-free imaging of human skin and oral mucosa equivalents. *Methods Mol Biol* 2020; 2150: 195–212.
31. Ingendoh-Tsakmakidis A, Eberhard J, Falk CS, et al. In vitro effects of *Streptococcus oralis* biofilm on peri-implant soft tissue cells. *Cells* 2020; 9: 1226.
32. Gong T, He X, Chen J, et al. Transcriptional profiling reveals the importance of RcrR in the regulation of multiple sugar transportation and biofilm formation in *Streptococcus mutans*. *mSystems* 2021; 6: e0078821.
33. Klanliang K, Asahi Y, Maezono H, et al. An extensive description of the microbiological effects of silver diamine fluoride on dental biofilms using an oral in situ model. *Sci Rep* 2022; 12: 7435.
34. Hartmann A, Boukamp P and Friedl P. Confocal reflection imaging of 3D fibrin polymers. *Blood Cells Mol Dis* 2006; 36: 191–193.
35. Pereira AR, Trivanović D, Stahlhut P, et al. Preservation of the naïve features of mesenchymal stromal cells in vitro: comparison of cell- and bone-derived decellularized extracellular matrix. *J Tissue Eng* 2022; 13: 20417314221074453.
36. Sriram G, Bigliardi PL and Bigliardi-Qi M. Fibroblast heterogeneity and its implications for engineering organotypic skin models in vitro. *Eur J Cell Biol* 2015; 94: 483–512.
37. Frevert CW, Felgenhauer J, Wygrecka M, et al. Danger-associated molecular patterns derived from the extracellular matrix provide temporal control of innate immunity. *J Histochem Cytochem* 2018; 66: 213–227.
38. Tomlin H and Piccinini AM. A complex interplay between the extracellular matrix and the innate immune response to microbial pathogens. *Immunology* 2018; 155: 186–201.
39. Scheibner KA, Lutz MA, Boodoo S, et al. Hyaluronan fragments act as an endogenous danger signal by engaging TLR2. *J Immunol* 2006; 177: 1272–1281.
40. Hsieh JY, Smith TD, Meli VS, et al. Differential regulation of macrophage inflammatory activation by fibrin and fibrinogen. *Acta Biomater* 2017; 47: 14–24.
41. García-García A and Martin I. Extracellular matrices to modulate the innate immune response and enhance bone healing. *Front Immunol* 2019; 10: 2256.
42. Rowley AT, Nagalla RR, Wang SW, et al. Extracellular matrix-based strategies for immunomodulatory biomaterials engineering. *Adv Healthc Mater* 2019; 8: e1801578.
43. Shang L, Deng D, Buskermolen JK, et al. Commensal and pathogenic biofilms alter toll-like receptor signaling in reconstructed human gingiva. *Front Cell Infect Microbiol* 2019; 9: 282.
44. Baek KJ, Choi Y and Ji S. Gingival fibroblasts from periodontitis patients exhibit inflammatory characteristics in vitro. *Arch Oral Biol* 2013; 58: 1282–1292.
45. Han X and Amar S. Identification of genes differentially expressed in cultured human periodontal ligament fibroblasts vs. human gingival fibroblasts by DNA microarray analysis. *J Dent Res* 2002; 81: 399–405.
46. Sliopen I, Van Damme J, Van Essche M, et al. Microbial interactions influence inflammatory host cell responses. *J Dent Res* 2009; 88: 1026–1030.
47. Uchida Y, Shiba H, Komatsuzawa H, et al. Expression of IL-1 beta and IL-8 by human gingival epithelial cells in response to *Actinobacillus actinomycetemcomitans*. *Cytokine* 2001; 14: 152–161.
48. Wang PL, Oido-Mori M, Fujii T, et al. Heterogeneous expression of toll-like receptor 4 and downregulation of toll-like receptor 4 expression on human gingival fibroblasts by *Porphyromonas gingivalis* lipopolysaccharide. *Biochem Biophys Res Commun* 2001; 288: 863–867.
49. Liu J, Wang Y and Ouyang X. Beyond toll-like receptors: *Porphyromonas gingivalis* induces IL-6, IL-8, and VCAM-1 expression through NOD-mediated NF- κ B and ERK signaling pathways in periodontal fibroblasts. *Inflammation* 2014; 37: 522–533.
50. Souza PPC, Lundberg P, Lundgren I, et al. Activation of toll-like receptor 2 induces B1 and B2 kinin receptors in human gingival fibroblasts and in mouse gingiva. *Sci Rep* 2019; 9: 2973.
51. Uehara A and Takada H. Functional TLRs and NODs in human gingival fibroblasts. *J Dent Res* 2007; 86: 249–254.
52. Wang PL, Azuma Y, Shinohara M, et al. Toll-like receptor 4-mediated signal pathway induced by *Porphyromonas gingivalis* lipopolysaccharide in human gingival fibroblasts. *Biochem Biophys Res Commun* 2000; 273: 1161–1167.
53. Round JL, Lee SM, Li J, et al. The toll-like receptor 2 pathway establishes colonization by a commensal of the human microbiota. *Science* 2011; 332: 974–977.
54. Behm C, Blufstein A, Abhari SY, et al. Response of human mesenchymal stromal cells from periodontal tissue to LPS depends on the purity but not on the LPS source. *Mediators Inflamm* 2020; 2020: 8704896.
55. Abranches J, Zeng L, Kajfasz JK, et al. Biology of oral streptococci. *Microbiol Spectr* 2018; 6: 10.1128/microbiol-spec.GPP3-0042-2018
56. Kabe Y, Ando K, Hirao S, et al. Redox regulation of NF-kappaB activation: distinct redox regulation between the cytoplasm and the nucleus. *Antioxid Redox Signal* 2005; 7: 395–403.
57. Herrero ER, Slomka V, Bernaerts K, et al. Antimicrobial effects of commensal oral species are regulated by environmental factors. *J Dent* 2016; 47: 23–33.
58. Jeffery V, Goldson AJ, Dainty JR, et al. IL-6 signaling regulates small intestinal crypt homeostasis. *J Immunol* 2017; 199: 304–311.
59. Sriram G, Alberti M, Dancik Y, et al. Full-thickness human skin-on-chip with enhanced epidermal morphogenesis and barrier function. *Mater Today* 2018; 21: 326–340.
60. Shah P, Fritz JV, Glaab E, et al. A microfluidics-based in vitro model of the gastrointestinal human-microbe interface. *Nat Commun* 2016; 7: 11535.
61. Kim HJ, Lee J, Choi JH, et al. Co-culture of living microbiome with microengineered human intestinal villi in a gut-on-a-chip microfluidic device. *J Vis Exp* 2016; 114: 54344.
62. Ramadan Q and Ting FC. In vitro micro-physiological immune-competent model of the human skin. *Lab Chip* 2016; 16: 1899–1908.
63. Kim HJ, Li H, Collins JJ, et al. Contributions of microbiome and mechanical deformation to intestinal bacterial overgrowth and inflammation in a human gut-on-a-chip. *Proc Natl Acad Sci USA* 2015; 113: E7–E15.